REPORT DOCUMENTATION PAGE

Form Approved
OMB No. 0704-0188

1. REPORT DATE *(DD-MM-YYYY)*	2. REPORT TYPE	3. DATES COVERED *(From - To)*
31-10-2004	Final Report	May 1 2004 - October 31 2004

4. TITLE AND SUBTITLE
Energy Finite Element Analysis System

5a. CONTRACT NUMBER
N00014-04-M-0123

5b. GRANT NUMBER

5c. PROGRAM ELEMENT NUMBER

6. AUTHOR(S)
Nickolas Vlahopoulos

5d. PROJECT NUMBER

5e. TASK NUMBER

5f. WORK UNIT NUMBER

7. PERFORMING ORGANIZATION NAME(S) AND ADDRESS(ES)
Michigan Engineering Services, LLC.
3916 Center Trade Drive
Ann Arbor, MI 48108

8. PERFORMING ORGANIZATION REPORT NUMBER
MES-ONR-SBIR-I-1

9. SPONSORING/MONITORING AGENCY NAME(S) AND ADDRESS(ES)
Office of Naval Research
Dr. Luise Couchman, ONR 334
Ballston Tower One
800 North Quincy Street
Arlington, VA 22217-5660

10. SPONSOR/MONITOR'S ACRONYM(S)
ONR

11. SPONSORING/MONITORING AGENCY REPORT NUMBER

12. DISTRIBUTION AVAILABILITY STATEMENT
Unlimited/Unclassified

13. SUPPLEMENTARY NOTES

20041108 170

14. ABSTRACT

This report was developed under SBIR contract award for Solicitation topic #N04-132
New Naval initiatives, like the DD(X) program, impose stringent noise and vibration targets, and require assessment and reduction of noise due to machinery, flow, and propulsion. A typical surface ship structure exhibits thousands of normal modes below 30Hz. Thus, the frequency range of interest from signature and hull vibration objectives extends far beyond what existing finite element based methods can predict. High noise levels in living quarters and in working spaces due to acoustic emissions from machinery and operating aircraft creates habitability concerns which must also be addressed in new surface ship designs. Recently, an Energy Finite Element Analysis (EFEA) and an Energy Boundary Element Analysis (EBEA) formulation have been developed by the PI of this project, and they have been applied for computing the vibration of submersible vehicles and the associated radiated noise at frequencies beyond the limits of conventional finite element methods. In addition to the Naval applications the EFEA and EBEA methods have been applied successfully in predicting vibration and acoustic fields in aerospace and automotive applications. The Phase I effort of this project established key capabilities for the EFEA and EBEA system for analyzing full scale surface ships and submarines in a robust and user friendly manner.

Energy Finite Element Analysis System
SBIR topic N04-132, Final Report 0001AC

Navy Small Business Innovation Research Program

Submitted to: **Office of Naval Research**

Contract Number N00014-04-M-0123

Submitted by:

Michigan Engineering Services, LLC

3916 Trade Center Drive

Ann Arbor, MI 48108

Period covered by this report: May 1, 2004 - October 31, 2004

1. Significance of the Phase I Work and relevancy with the Phase II effort

New Naval initiatives, like the DD(X) program, impose stringent noise and vibration targets, and require the assessment and the reduction of noise due to machinery, flow, and propulsion. A typical surface ship structure exhibits thousands of normal modes below 30Hz. Thus, the frequency range of interest from signature and hull vibration objectives extends far beyond what conventional finite element computational methods can predict. Lower noise requirements for surface ship silencing, along with stringent vibration specifications, and the utilization of new materials for ship construction, impose a significant challenge in modern ship design. High noise levels in living quarters and in working spaces due to acoustic emissions from machinery and operating aircraft creates habitability concerns which must also be addressed in new surface ship and aircraft carrier designs. High noise levels deteriorate the performance of a crew, reduce the permitted amount of time for a crew shift due to exposure to high noise levels, and lead to hearing loss due to exposure to noise over extended time periods. [1-5] Thus, in addition to the acoustic signature concerns, assessment and reduction of interior noise levels is also very important. The Phase I effort established the technical foundation for developing simulation tools which can be used by ship designers for meeting these stringent signature goals, interior noise levels, and vibration requirements.

The completed Phase I effort was based on an Energy Finite Element Analysis (EFEA) and an Energy Boundary Element Analysis (EBEA) formulation which have been developed in the past by the PI of this project [6-12]. The EFEA/EBEA formulations were validated in the past by computing the noise radiated from a large scale submersible vehicle, as a result of Turbulent Boundary Layer (TBL) excitation. The results of these analytical assessments have compared favorably with test data taken on the model during evaluation at the Naval Surface Warfare Center - Acoustic Research Detachment (NSWC-ARD). In addition to the Naval applications the EFEA and EBEA methods have been applied successfully in predicting vibration and acoustic fields in aerospace and automotive applications. In these fields vibration and noise levels are associated with passenger comfort, perceived product quality, and government regulations (e.g. environmental noise, pass-by noise). In the aerospace field the NASA Langley aluminum test-bed cylinder [16] has been analyzed using the EFEA and the results have been correlated to test data. Excitation was applied through shakers at four different locations on the structure and the induced structural vibration was measured. The test data were compared to the EFEA results. Figure 1 presented the magnitude of the difference between the test data and EFEA results for the vibrational energy in forty bays of the cylinder. The results are averaged over all 1/3 octave bands between 315Hz and 6,300Hz. The maximum difference is 2.4dB. Thus, very good correlation is observed, and the EFEA method is validated for analyzing aircraft type of structures.

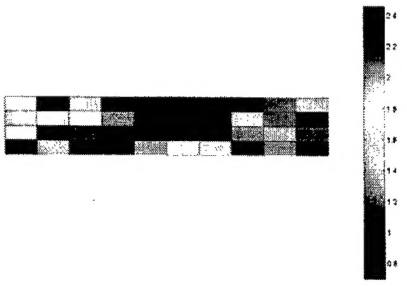

Figure 1. Frequency averaged difference between test data and EFEA in dB

In automotive applications the EBEA development of Phase I effort has been utilized for computing the acoustic field around a vehicle for multiple air-borne noise sources and over the frequency range 630Hz – 8,000Hz. The EBEA results have been validated through comparison to test data collected in a semi-anechoic test cell. General Motors Corporation is processing the purchase order for a license of the EBEA code developed as part of the work of the Phase I project.

Up to this point the PI has developed the following computational capabilities in the EFEA and EBEA areas:[6-15]

(i) A joint formulation has been developed for multiple plates connected together with or without a stiffener at the connection.[12]
(ii) Capability to automatically define joints at multiple connections between plates.
(iii) Accounting for heavy fluid loading effects in a fully submerged structure. The added mass effect and the radiation damping have been included in the EFEA formulation. The added mass effect has also been included in the derivation of the power transfer coefficients.[8,11]
(iv) A hybrid formulation has been developed for cylindrical structures with periodic stiffeners in the circumferential direction.[11]
(v) An internal re-numbering scheme has been incorporated in the EFEA solver for bandwidth minimization.
(vi) The EBEA has been developed for high frequency acoustic radiation.[10]
(vii) A hybrid formulation has been developed for modeling periodic axial and circumferential stiffeners without heavy fluid loading.
(viii) Interior acoustic elements have been developed in the EFEA for computing interior noise levels.
(ix) A joint formulation has been developed between interior acoustic elements and structural plate elements for interior acoustic analysis.
(x) A hybrid FEA formulation has been developed for automotive types of applications.[13,14]

Thus far, the energy developments have been validated through:

(i) Comparison of EFEA and EBEA results to very dense conventional finite element analyses.[6,9]
(ii) Comparison between EFEA results and statistical energy analysis.[6]
(iii) Correlation to test data in an underwater application for a large scale vehicle.
(iv) Correlation to test data for the NASA aluminum test-bed cylinder.
(v) Correlation to test data for air-borne automotive applications.[15]

During the Phase I effort of this project the following tasks were completed:

(i) Development and validation of an EFEA formulation for partial fluid loading on the structure.
(ii) Modeling and validation of the free surface effects in acoustic radiation.
(iii) Development and validation of a multi-domain EBEA formulation for modeling the effects of a mixed phase acoustic medium in acoustic radiation.

The Phase I effort established the foundation for pursuing the development of a complete Energy Finite Element Analysis System, suitable for analyzing full scale Naval structures. In order to develop such a system it is necessary to develop computational capabilities which allow handling models with a large number of elements, making the software user friendly, and validating the developed codes for problems of interest to the Navy. The following list of potential tasks can be pursued during a Phase II effort:

- Matrix partitioning and sub-structuring within a parallel solver environment. The new solver technology can be applied to both the EFEA and the multi-zone EBEA solvers. The new codes will be tested that they can solve the size of meaningful problems which are of interest to the Naval shipbuilding community.

- Develop a user-friendly capability within the pre-EFEA code developed during the Phase I effort, which will allow to automatically divide a model into substructures, identify the wetted elements associated with each substructure, and define properly the joints within each substructure.

- Implement in the EFEA solver the rational functional approximation approach developed at NSWC-Carderock. This will provide an opportunity to include in the Naval/EFEA code recent technology developed by the Navy. Such implementation will provide more computational alternatives to the Naval user community.

- Embed within the EFEA solver the capability for computing power transfer coefficients from periodic structure theory.

- Interaction and collaboration with Northrop Grumman Newport News in order to validate the Phase II developments, and in order to ensure that the final product can handle the analysis of full scale Naval models.

- Develop an interface between the EFEA and EBEA solvers with the LMS/Virtual Lab. This development can take advantage of the existing pre and post-processing capabilities of the Virtual Lab in order to provide a powerful way of visualizing the results from an EFEA/EBEA analysis.

- Develop a database of validation cases which will summarize all the previous and all of the on-going efforts where test data were compared to EFEA and EBEA analyses. The corresponding data files and results files will serve as sample problems in order to promote the new technology developed by this SBIR project.

- Develop documentation, manuals, and presentation material for the codes developed under this SBIR project in order to promote their use within the Naval community.

2. Backround information on the EFEA and EBEA methods

Since this SBIR project is based on the EFEA and EBEA methods, technical information about these two methods is briefly reviewed first. Then, the technical information associated with the completed Phase I tasks is presented in the Section 3.

2.1. Technical Background on EFEA formulation with heavy fluid loading [6-9,11,12]

Although several developments have been completed, and several types of elements and joints are available in the EFEA library, only the information on plate elements and plate joints under heavy fluid loading is presented here. The EFEA governing differential equation for the flexural energy density of a plate under heavy fluid loading is:

$$-\frac{(c_g)_{eff}^2}{\eta\omega}\nabla^2 <\underline{e}> +\eta\omega<\underline{e}> = <\underline{\Pi}_{in}> \tag{1}$$

where $(c_g)_{eff} = 2*\sqrt[4]{\frac{D}{m_{eff}}\omega^2}$ is the effective group velocity of plate under heavy fluid loading, and η is the total damping coefficient which includes both the structural damping and the radiation damping. Compared to the EFEA governing differential equation in vacuum, the effective group velocity instead of the normal group velocity and the total damping factor instead of the structural damping factor are used in equation (1). The radiation damping for a heavy fluid is based on Rummerman's work. [17,18] A finite element formulation is employed for solving equation (1) numerically.

In the EFEA formulation, the energy density is discontinuous at connections between members. A joint matrix derived from the power transfer coefficients is utilized for coupling the energy density variables across a joint. The power transfer coefficients are evaluated from analytical solutions of semi-infinite members that demonstrate the same structural characteristics with the components for which the power transfer coefficients are computed. The complete set of transmission coefficients for a joint is written in the form $[\tau]_{eff}$ where subscript "eff" indicates that the heavy fluid loading effect is included in the derivation. The joint matrices in the EFEA formulation define the power transfer across elements at the joints and are derived from the power transfer coefficients:

$$[J]_{eff} = ([I]-[\tau]_{eff})([I]+[\tau]_{eff})^{-1}\int_B \phi_i\phi_j dB \tag{2}$$

where ϕ_i, ϕ_j are Lagrangian basis functions, and B is the boundary area between elements i and j at the joint. Thus, the fluid loading effects are finally included in the derivation of the joint matrices and in the power transfer mechanism in the EFEA system of equations. The final system of EFEA equations is obtained from the finite element form of equation (1) and from equation (2):

$$[[E]_{eff} + \sum[J]_{eff}]\{<\underline{e}>\} = \{f\} \tag{3}$$

where $[E]_{eff}$ is the system matrix derived from left hand side of equation (1), $\{f\}$ is the vector related to input power in equation (1), and Σ indicates the addition of the joint matrices that correspond to all the joints in the model to the EFEA system matrix $[E]_{eff}$.

2.2 Technical background on EBEA [10]

The EBEA allows to calculate the radiated noise from the EFEA results. The EFEA analysis computes the structural vibration, and for the elements which are in contact with the surrounding fluid it also computes the acoustic power radiated into the fluid domain. The EBEA analysis uses as boundary conditions the results for the radiated power on the outer surface of a model and computes the acoustic propagation in the field. The original EBEA formulation developed for acoustic radiation in an unbound medium is overviewed here.

The Green's functions that are utilized in the EBEA formulation are based on an unbound medium. The acoustic pressure at any field point Y exterior to the structure is expressed as:

$$\hat{p}_{\mathrm{Y}} = \int_S A(\mathrm{P}) g(\mathrm{P},\mathrm{Y}) \mathrm{d}S \tag{4}$$

where S is the surface of the structure, P denotes the point located on the surface S, $A(\mathrm{P})$ is the complex source strength amplitude at P, and $g(\mathrm{P},\mathrm{Y}) = \dfrac{e^{-ikr}}{4\pi r}$ is the Green's function for three dimensional infinite system, r is the distance between points P and Y, and k is the wavenumber. The acoustical velocity vector is obtained from the acoustic pressure

$$\hat{\mathbf{v}}_{\mathrm{Y}} = -\frac{1}{\mathrm{i}\omega\rho}\nabla\hat{p}_{\mathrm{Y}} = -\frac{1}{\mathrm{i}\omega\rho}\int_S A \nabla g(\mathrm{P},\mathrm{Y}) \mathrm{d}S \tag{5}$$

Equations (17) and (18) are employed for developing expressions for the ensemble averaged quantities $\mathrm{E}\left[\hat{p}_{\mathrm{Y}}\hat{p}_{\mathrm{Y}}^*\right]$, $\mathrm{E}\left[\hat{\mathbf{v}}_{\mathrm{Y}}\cdot\hat{\mathbf{v}}_{\mathrm{Y}}^*\right]$ and $\mathrm{E}\left[\hat{p}_{\mathrm{Y}}\hat{\mathbf{v}}_{\mathrm{Y}}^*\right]$. The latter expressions are introduced in the equations for the frequency averaged acoustic energy density and intensity:

$$\tilde{e}_{\mathrm{Y}} = \mathrm{E}\left[\langle e_{\mathrm{Y}}\rangle\right] = \frac{1}{4}\left[\rho\mathrm{E}\left[\hat{\mathbf{v}}_{\mathrm{Y}}\cdot\hat{\mathbf{v}}_{\mathrm{Y}}^*\right] + \frac{1}{\rho c^2}\mathrm{E}\left[\hat{p}_{\mathrm{Y}}\hat{p}_{\mathrm{Y}}^*\right]\right] \text{ and } \tilde{\mathbf{I}}_{\mathrm{Y}} = \mathrm{E}\left[\langle \mathbf{I}_{\mathrm{Y}}\rangle\right] = \frac{1}{2}\mathrm{Re}\left(\mathrm{E}\left[\hat{p}_{\mathrm{Y}}\hat{\mathbf{v}}_{\mathrm{Y}}^*\right]\right) \tag{6}$$

Then the equations for the primary variables of the EBEA formulation are developed:

$$\tilde{e}_{\mathrm{Y}} = \int_S \sigma(\mathrm{P})\left(\frac{\rho}{64\pi^2 r^4} + \frac{k^2\rho}{32\pi^2 r^2}\right)\mathrm{d}S \text{ and } \tilde{\mathbf{I}}_{\mathrm{Y}} = \int_S \sigma(\mathrm{P})\frac{k^2\rho c}{32\pi^2 r^2}\mathbf{E}_r \mathrm{d}S \tag{7}$$

where $\sigma(\mathrm{P})$ the strength density of the energy source placed at point P of the surface of the model. Since the acoustic power radiated from each element of the structure in contact with the heavy fluid is known from the EFEA analysis, the corresponding acoustic intensity for each element is computed by dividing the power with the corresponding area of each element. Then, by placing the field point Y on each one of the elements of the model and by requiring for the acoustic intensity to be equal to the prescribed intensity a square system of equations is generated and the source strengths $\sigma(\mathrm{P})$ for all the distributed acoustic sources are computed.

3. Technical Developments during the Phase I effort

3.1 EFEA formulation for partial heavy fluid loading on the structure

This work developed the following computational capabilities:

- automated identification of outer wetted elements
- added mass and radiation damping only on wetted elements
- derivation of power transfer coefficients

The user provides the EFEA model of a ship in NASTRAN format (which any commercial pre and post-processor can generate). The user also provides the definition of the waterline plane in terms of a point in space and an orientation perpendicular to the waterline plane. A pre-EFEA code was developed in this project. The new code allows to automatically identify:

- All of the joints in the model
- The most outer elements of the hull of the ship model below the waterline and in contact with the heavy fluid medium

When joints are identified between elements, the elements are automatically disconnected by generating appropriate new nodes and appropriate cards are generated in the output data file which is used by the EFEA solver for the analysis. When elements are identified as wetted elements their property ID number in the EFEA model file changes from its original value in order to indicate contact with heavy fluid. Any element which is in contact with heavy fluid is subjected to the added mass and the radiation damping effects during the EFEA computations performed by the EFEA solver.

As a validation example for the correct identification of the joints the EFEA model of a fishing vessel is analyzed by the pre-EFEA code. Figure 2 presents half of the EFEA model of a fishing vessel in order for the internal components to be visible.

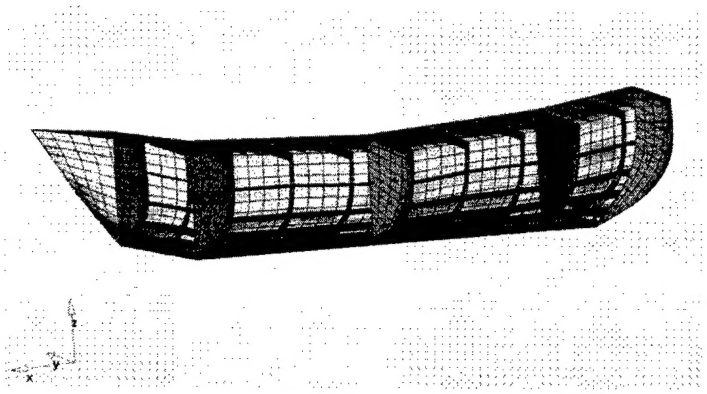

Figure 2. Half of the EFEA model of a fishing vessel

The EFEA model for this vessel comprises the input to the new pre-EFEA code. The pre-EFEA code introduces automatically the necessary changes for the joints (at all the locations of geometric discontinuity, intersections between stiffeners and the hull, and intersections between the bulkheads and the hull in this model), and it identifies only the outer elements of the hull which are below the waterline as wetted elements. Figure 3 presents all the joints and the free edges in the model after it is modified by the pre-EFEA code.

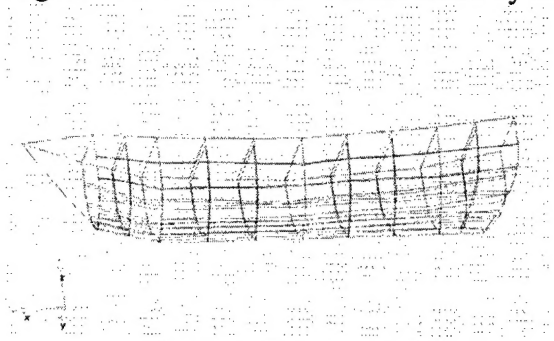

Figure 3. Joints and free edges in the EFEA model after the pre-EFEA code

Figure 4 presents the outer elements of the hull which are identified as wetted elements by the pre-EFEA code. The code can differentiate between outer elements of the hull and all the internal elements of the stiffeners and the bulkheads, and it automatically assigns the heavy fluid loading only on the former.

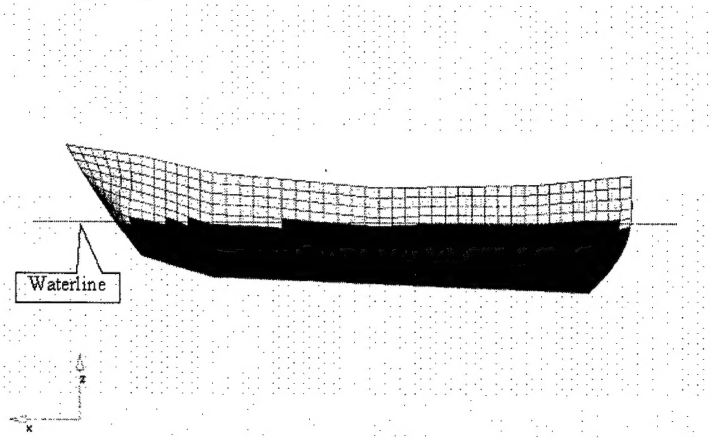

Figure 4. Wetted elements identified by the pre-EFEA code

3.2 Validation of the EFEA formulation for partial fluid loading on the structure

The validation for the correct identification of the joints and the wetted elements is performed by inspecting the model after the pre-EFEA code in order to make certain that the joints and the wetted elements have been identified automatically in the locations where they are supposed to be placed. Figure 5 presents a typical summary of the operations performed by the pre-EFEA code.

```
            Summary of P-P Joints
Number of elements in the model:        366
Number of original nodes in the model:   390
Number of original nodes eliminated:     143
Number of added nodes for joints:        339
Number of total final nodes :            586
Number of total joints generated:        156
Number of joints connect 2 elements:     136
Number of joints connect 3+ elements:     20
            Summary of Wetted Elements
Elements with the following Property IDs are wetted:
 PID =   4
 PID =   6
```

Figure 5. Sample output summary from the pre-EFEA code

Figure 5 summarizes the new nodes and the joints which were created in the model, the type of joints which were created and the changes which were made in the properties of certain elements in order to represent the fact that the elements with the updated properties are in contact with exterior fluid. Figure 6 presents a typical section of the data file which comprises the input to the pre-EFEA code, and Figure 7 presents a typical section of the modified data file produced by the pre-EFEA code.

```
GRID       1      0.0    1.1974290.1524
GRID       2      0.635  0.8708570.0
GRID       3      0.635  0.3265710.0
....
CQUAD4       1     1     1   179    170    181
CQUAD4       2     1   179    98    171    170
CQUAD4       3     1    98    14    388    171
CQUAD4       4     1    83   348    125    138
....
```

Figure 6. Typical section of the data file used as input in the pre-EFEA code

```
GRID       1         0.0 1.19743 .152400
GRID       3      .635000 .326571   0.0
GRID       4      .254000 .108857   0.0
.....
CQUAD4       1     4     1   179    391    392
CQUAD4       2     4   179    98    395    391
CQUAD4       3     4    98   399    400    395
CQUAD4       4     1    83   348    125    138
.....
PJOINT       2
     1   391    392
   258   393    394
.....
PJOINT       3
   287   977    835
   290   978    746
   366   980    744
.....
PLATE     1  0.005    1 0 0.0 0.0 0.0 0 0 0.0 0 0 0.0 0.0 0.0
PLATE     2  0.005    2 0 0.0 0.0 0.0 0 0 0.0 0 0 0.0 0.0 0.0
PLATE     4  0.005    1 1 L_a L_b 0.0 PACOUS_ID 0.0 0 0 0.0 0.0 0.0
PLATE     6  0.005    3 1 L_a L_b 0.0 PACOUS_ID 0.0 0 0 0.0 0.0 0.0
MPLATE    1  0.2070E+12 7800.000   0.330 0.0 0.0 0.0
MPLATE    2  0.2070E+12 7800.000   0.330 0.0 0.0 0.0
MPLATE    3  0.2070E+12 7800.000   0.330 0.0 0.0 0.0
```

Figure 7. Typical section of the modified data file produced as output by the pre-EFEA code

As it can be observed in Figure 7, additional cards are introduced automatically in the file in order to define the joints. In addition, new material properties (properties 4 and 6) are created and are associated with the elements which are identified to be in contact with the external fluid. The development of the pre-EFEA code makes a very tedious manual process seamless for a user and enables the easy analysis for naval ship structures.

The proper implementation of the partial fluid loading in the EFEA code, and the proper transmission of the information from the pre-EFEA code to the EFEA solver are demonstrated through comparison between EFEA solutions and conventional dense FEA/IFEA models for a representative scaled down section of a generic surface ship structure, presented in Figures 8, 9, and 10. The main dimensions of the structure are presented in Figure 9. A longitudinal bulkhead divides the structure into two sections and six transverse stiffeners define seven bays in each half.

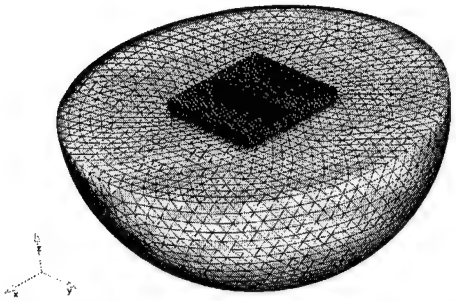

Figure 8. FEA/IFEA model for representative section of a surface ship structure (49,689 fluid elements)

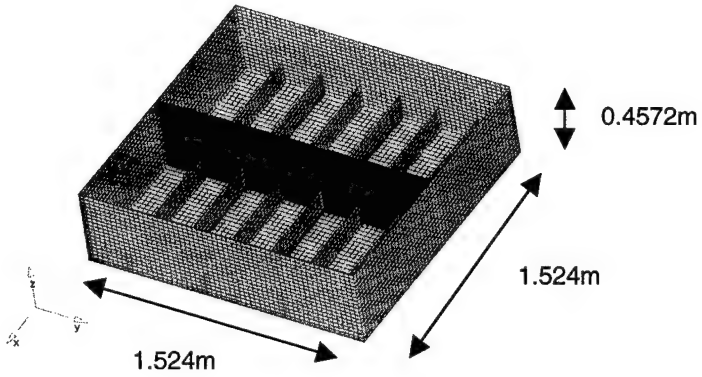

Figure 9. FEA structural model for representative section of surface ship structure (10,192 structural elements)

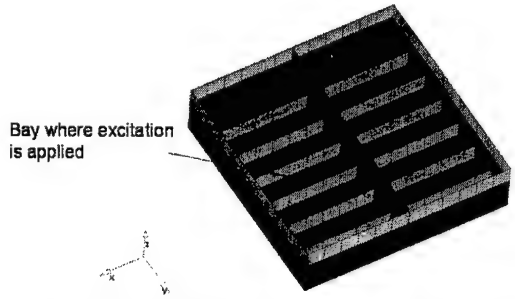

Figure 10. EFEA model for representative section of a surface ship structure (includes heavy fluid loading effects, 438 elements)

Excitation is applied at one of the middle bays as depicted in Figure 10 and the vibration induced to all the other bays is computed. In the FEA/IFEA method the results for the energy density are space averaged over each bay and then frequency averaged over each 1/3 octave band, in order to compute the average flexural energy for each bay at each 1/3 octave band. The frequency range where the results are compared between the EFEA and the FEA/IFEA are at 1,600Hz, 2,000Hz and 2,500Hz. These frequency ranges are selected based on the size of the model and the dimensions of the structural members in order for both methods to provide accurate results. The results for the ratio (in dB values) between the energy density at each bay of the model vs. the energy density in the bay where the excitation is applied are presented in Figure 11.

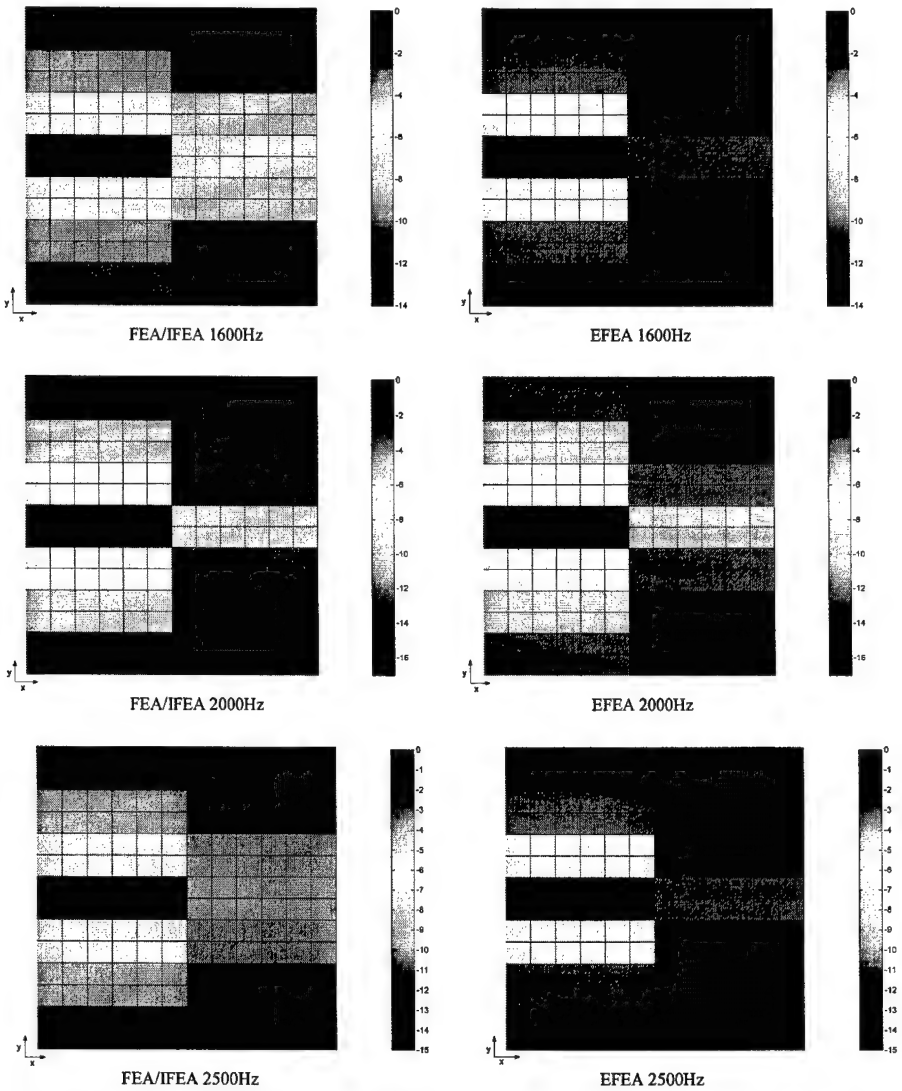

Figure 11. FEA/IFEA and EFEA results for the energy density ratio

Very good correlation is observed in the predictions for the vibrational energy between the two methods, thus validating the EFEA simulation results with the partial fluid loading effects.

3.3 Modeling the effects of a free surface in the acoustic radiation

A half-space boundary condition is introduced in the EBEA formulation in order to account for the presence of the half-space. The original Green's function has been modified to:

$$g(\mathrm{P},\mathrm{Y}) = e^{-ikr}/4\pi r - e^{-ikr_1}/4\pi r_1 \qquad (8)$$

where Y is a field point, P is an integration point, r is the distance between points P and Y, and r_1 is the distance between points Y and P_1 (P_1 is a point symmetric to point P with respect to the halfspace). The Green's function in Equation (8) corresponds to a pressure release boundary condition. It is employed in the equations for the acoustic pressure and the acoustic velocity (Equations 4 and 5, respectively) instead of the free field Green's function. The equations for the ensemble averaged quantities $\mathrm{E}\left[\hat{p}_\mathrm{Y}\hat{p}_\mathrm{Y}^*\right]$, $\mathrm{E}\left[\hat{\mathbf{v}}_\mathrm{Y}\cdot\hat{\mathbf{v}}_\mathrm{Y}^*\right]$ and $\mathrm{E}\left[\hat{p}_\mathrm{Y}\hat{\mathbf{v}}_\mathrm{Y}^*\right]$ become:

$$E[\hat{p}_Y \hat{p}_Y^*] = \int_S \mu(P) |A(P)|^2 \left(\frac{1}{16\pi^2 r^2} + \frac{1}{16\pi^2 r_1^2}\right) dS \tag{9}$$

$$E[\hat{\mathbf{v}}_Y \hat{\mathbf{v}}_Y^*] = \frac{1}{\omega^2 \rho^2} \int_S \mu(P) |A(P)|^2 \left(\frac{1}{16\pi^2 r^4} + \frac{1}{16\pi^2 r_1^4} + \frac{k^2}{16\pi^2 r^2} + \frac{k^2}{16\pi^2 r_1^2}\right) dS \tag{10}$$

$$E[\hat{p}_Y \hat{\mathbf{v}}_Y^*] = \frac{1}{\omega\rho} \int_S \mu(P) |A(P)|^2 \left(\frac{1}{16\pi^2 r^3}(i + kr)\,\mathbf{E}_r + \frac{1}{16\pi^2 r_1^3}(i + kr_1)\mathbf{E}_{r_1}\right) dS \tag{11}$$

By defining the source strength $\sigma(P)$ at the surface point P on the boundary element model as:

$$\sigma(P) = \frac{\mu(P) |A(P)|^2}{\rho^2 \omega^2} \tag{12}$$

and by using Equations (6) for the definition of the frequency averaged acoustic energy density and intensity results into the final set of integral equations for the EBEA formulation:

$$\tilde{e}_Y = \int_S \sigma(P) \left(\frac{\rho}{64\pi^2 r^4} + \frac{k^2\rho}{32\pi^2 r^2} + \frac{\rho}{64\pi^2 r_1^4} + \frac{k^2\rho}{32\pi^2 r_1^2}\right) dS \tag{13}$$

$$\tilde{\mathbf{I}}_Y = \int_S \sigma(P) \left(\frac{k^2\rho c}{32\pi^2 r^2}\mathbf{E}_r + \frac{k^2\rho c}{32\pi^2 r_1^2}\mathbf{E}_{r_1}\right) dS \tag{14}$$

where $\mathbf{E}_r$, $\mathbf{E}_{r_1}$ are unit vectors associated with the directions defined between points (P, Y) and (P_1, Y) respectively. Equations (13) and (14) are the main EBEA equations when the half-space is considered. The half-space development is validated for acoustic radiation in heavy fluid medium through comparison to an analytical solution. The lower half of a cylinder presented in Figure 12 is considered to be immersed in heavy fluid, thus the half-space is considered to pass through a plane of symmetry of the cylinder. The EBEA model is comprised only by half of the cylinder as it can be depicted in Figure 12.

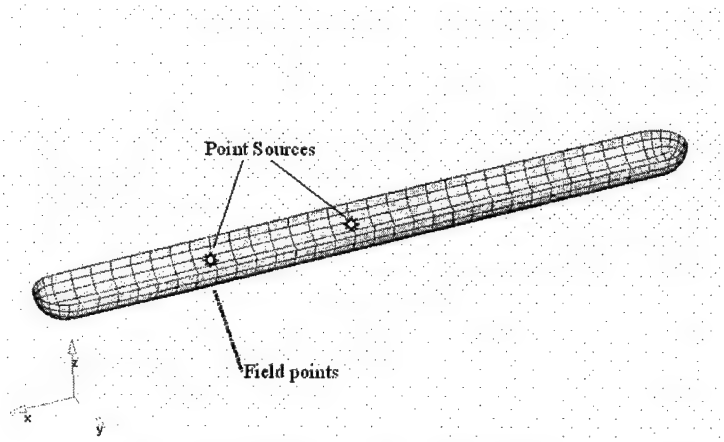

Figure 12. EBEA model of the lower half of a cylinder is immersed in heavy fluid

In order to develop the analytical solution, two point sources of unit strength are placed at the axis of the cylinder, and radiation in the half space is considered. The surface of the half-cylindrical radiator is considered originally as transparent. The acoustic energy density and intensity at any field point in the half space produced by the point sources are calculated using

the image method. The acoustic intensity on each element of the transparent surface is also calculated by the analytical formula using the image method. These values for the acoustic intensity comprise the boundary conditions for the half space EBEA computations. The distribution of energy sources is evaluated on the surface of the EBEA model from the boundary conditions. The surface results and Equations (13) and (14) are employed for calculating the acoustic energy density and intensity in the half space field. Computations for the one-third octave band of 3,000Hz are presented in Figures 13 and 14 for the acoustic energy density and the acoustic intensity, respectively, for the line of field points which is depicted in Figure 6 along with the EBEA model. The acoustic medium is considered to have speed of sound 1,500m/sec and density 1,000kg/m^3. Excellent correlation is observed between the EBEA and the analytical results.

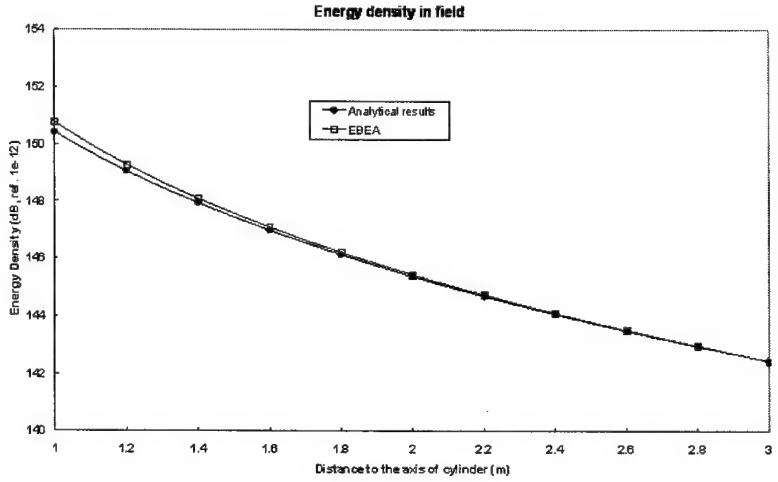

Figure 13. Acoustic energy density at field points, 3,000Hz one-third octave band

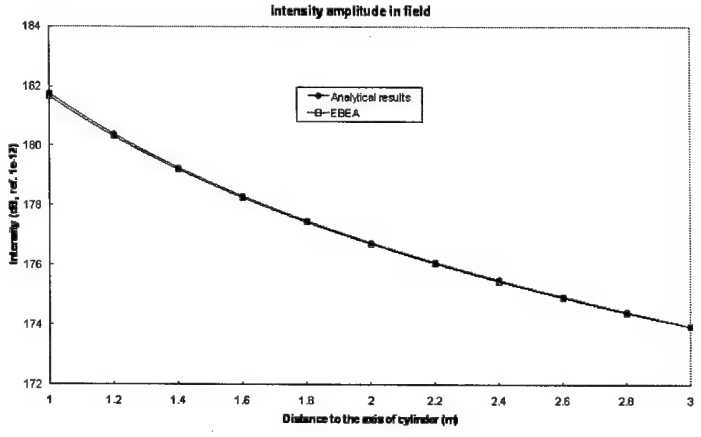

Figure 14. Magnitude of acoustic intensity at field points, 3,000Hz one-third octave band

3.4 Modeling the effects of a mixed phase acoustic medium in the acoustic radiation

The properties of the heavy acoustic medium (density and speed of sound) in the vicinity of a ship can be different compared to the remaining of the acoustic medium due to the mixed phase fluid which is created from the flow near the ship. In the past a multi-domain formulation has

been developed in the conventional boundary element method (BEM) in order to solve acoustic problems with non-homogeneous domains.[19-21] The conventional multi-domain BEM formulation has also been employed to solve problems of sound radiation from openings in enclosures and sound radiation from open ducts. In order to account for the mixed phase effects on the acoustic radiation a multi-domain formulation is developed for the EBEA. The new developments combine elements of the conventional multi-domain BEM, of the EBEA, and of the half-space formulation described in Section 1.5. The system of equations which results from utilizing the intensity boundary conditions and equation (14) is:

$$[S]\{\sigma\} = \{I\} \tag{15}$$

where $[S]$ is the system matrix which is generated when placing the field point Y on each one of the boundary elements, $\{I\}$ is the vector of the prescribed intensity boundary conditions, and $\{\sigma\}$ is the vector with the strengths of all the acoustic sources distributed over all the energy boundary elements. When considering multiple domains within the acoustic medium it is possible to solve for a set up like the one presented in Figure 15.

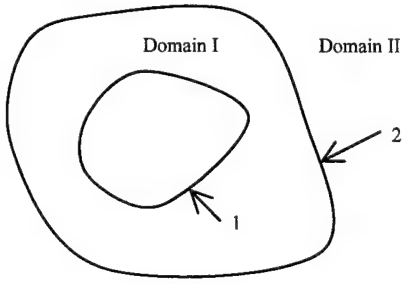

Figure 15. Configuration with two acoustic domains

In Figure 15 "I" and "II" indicate the two different domains. "1" indicates the boundary where the intensity boundary conditions are prescribed, and "2" is the interface between domains I and II. In the developed code it is possible to define several domains and have more than one domain in the vicinity of the ship (i.e. divide domain I of Figure 15 in several domains with different properties). For simplicity, the equations for a configuration with only two domains are presented here. The numerical system of equations for domain I is partitioned based on the boundaries "1" and "2", resulting in:

$$\begin{bmatrix} S_I^{11} & S_I^{12} \\ S_I^{21} & S_I^{22} \end{bmatrix} \begin{Bmatrix} \sigma_I^1 \\ \sigma_I^2 \end{Bmatrix} = \begin{Bmatrix} I_I^1 \\ I_I^2 \end{Bmatrix} \tag{16}$$

where superscript "1" and "2" are associated with the boundaries "1" and " 2" respectively. In a similar manner the EBEA equations for the domain II are:

$$[S_{II}^2]\{\sigma_{II}^2\} = \{I_{II}^2\} \tag{17}$$

Taking into account that at the interface the source strengths should be the same (i.e. $\{\sigma_I^2\} = \{\sigma_{II}^2\} = \{\sigma^2\}$), that the interface intensities should have opposite values due to the different orientation of the unit normal in domains I and II (i.e. $\{I_I^1\} = -\{I_{II}^2\}$), and by combining equations (16) and (17) results into the final system of equations for the multi-domain EBEA:

$$\begin{bmatrix} S_I^{11} & S_I^{12} \\ S_I^{21} & [S_I^{22} + S_{II}^2] \end{bmatrix} \begin{Bmatrix} \sigma_I^1 \\ \sigma^2 \end{Bmatrix} = \begin{Bmatrix} I_I^1 \\ 0 \end{Bmatrix} \tag{18}$$

Once Equation (18) is solved for the strengths of the sources on the boundary element model, the acoustic field is computed everywhere within the acoustic domains I and II.

In order to validate the new multi-domain EBEA development analytical solutions for acoustic radiation are compared to results from multi-zone EBEA analyses. The set-up for the first analysis is presented in Figure 16. The analytical solution generated from a single point source in the presence of a half-space is employed. The analytical solution allows computing the acoustic energy density anywhere in the field. It also allows computing the acoustic intensity on the surface of the inner hemisphere. The latter are used as the excitation boundary conditions for the multi-domain EBEA analysis. Although the material properties in this case are all of them the same, three different zones (Figure 16) are defined in order to test the multi-domain EBEA solution. The intensity boundary conditions are prescribed on the surface of the inner sphere and the acoustic energy density is computed both inside domains 2 and 3. Numerical results for the acoustic energy density in domains 1 and 3 are compared with the analytical solution in Figures 17 and 18, respectively.

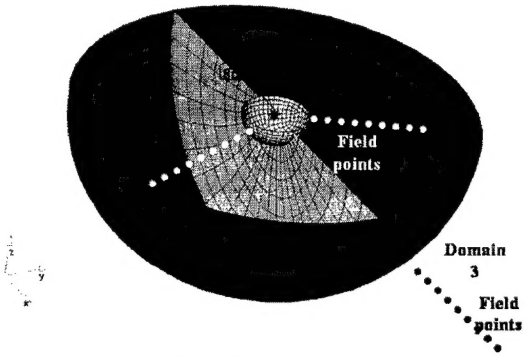

Figure 16. Set-up for multi-domain analysis using the analytical solution from a single source in a half-space

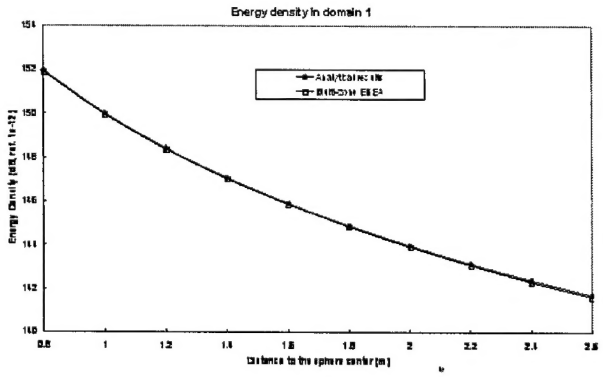

Figure 17. Numerical and analytical results for the energy density in Domain 1

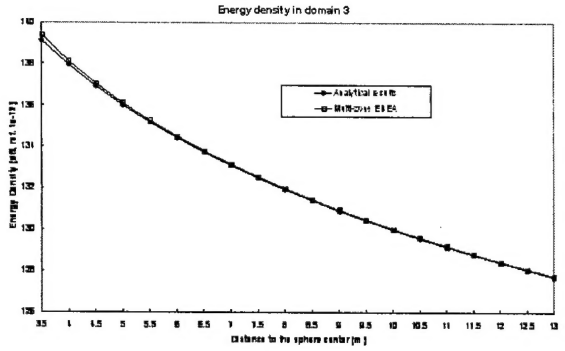

Figure 18. Numerical and analytical results for the energy density in Domain 3

In order to further test the new multi-domain EBEA capability a more complex set up is generated using the analytical solution for two point sources in a half-space (Figure 19). In this case the analytical solution is used to compute the acoustic energy density in the field and the acoustic intensity on the elements of the inner half-cylinder. During the analytical computation the half-cylinder is transparent. The computed intensity boundary conditions on the half-cylinder comprise the intensity boundary conditions for the multi-domain EBEA analysis. In this case 5 different domains are defined in the numerical model. Numerical results are compared with the analytical solution for the acoustic energy density at field points inside domains 3 and 5 (Figures 20 and 21, respectively).

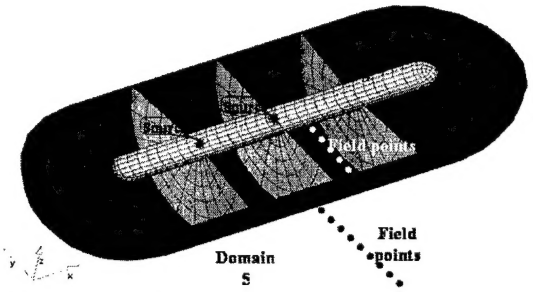

Figure 19. Set-up for multi-domain analysis using the analytical solution from two sources in a half-space

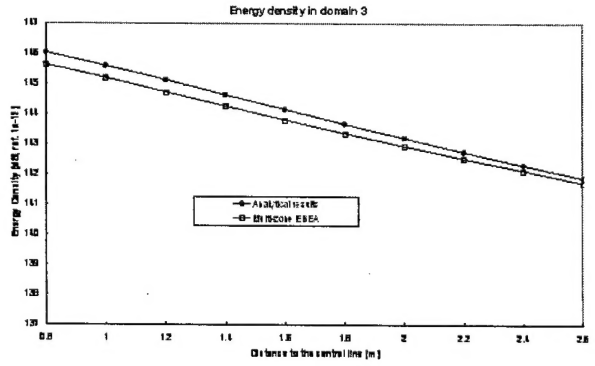

Figure 20. Numerical and analytical results for the energy density in Domain 3

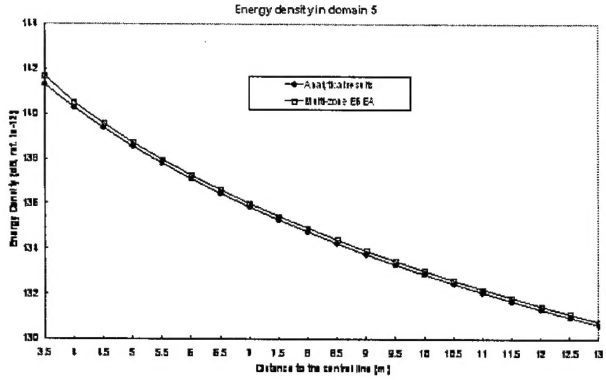

Figure 21. Numerical and analytical results for the energy density in Domain 5

Consistently good correlation is observed between all the numerical results and the analytical solutions.

4. Commercialization

The EFEA and the EBEA developments of this project will provide a general simulation system for analyzing full scale naval structures for acoustic signatures, habitability, and high frequency vibration induced due to loads from shock. All the Naval related simulation capabilities will comprise the Naval/EFEA&EBEA software system which will be marketed by MES to the US Naval Industry.

A separate product, with the capability to model only air as the acoustic medium (Air/EFEA&EBEA) will be marketed to the automotive aerospace, heavy construction equipment, and heavy vehicle industries. In all these applications high frequency excitation either from the engines, the road, or the external flow generates high frequency vibration on the vehicle structure and subsequently undesired interior noise. Since product quality is directly associated with the noise levels that the driver or the passengers are experiencing in a vehicle, there is a need for the Air/EFEA&EBEA product in these industries. General Motors Corporation has purchased the first commercial license of the EBEA code which was based on developments of this Phase I effort. GM's intent is to use the EBEA code in order to compute the noise field around a vehicle in air-borne noise applications.

LMS will act as a sales distributor for MES selling the Air/EFEA&EBEA product. LMS owns a worldwide network which specializes in sales of NVH products and services, both for test and simulation. The participation of LMS in this project as a commercialization partner ensures the commercial success and the financial sustenance of the work funded by this SBIR.

REFERENCES

1. Buiten, J., "Noise Exposure of Engine Room Personell," Proceedings of Internoise 1983, pp. 789-792.
2. Fisher, R. W., "Noise Control in a Large Tractor Tug," NOISE-CON '94, May 1994, pp. 709-714.
3. Jansen, J. H., "Hypothesis of Simultaneous Noise and Vibration Annoyance Rating in Shipboard Accomodation," Noise Control Engineering, Vol. 16, 1981, pp. 145-150.
4. SNAME T&R Bulletin 2-25, "ship Vibration and Noise Guidelines."

5. Tamure, Y., Kawada, T., and Sasazawa, Y., "Effect of Ship Noise on Sleep," Journal of Sound and Vibration, Vol. 205, No.4, 1997, pp. 417-425.
6. N. Vlahopoulos, L.O. Garza-Rios, and C. Mollo, "Numerical Implementation, Validation, and Marine Applications of an Energy Finite Element Formulation," *Journal of Ship Research*, Vol. 43, No. 3, Sept. 1999, pp. 143-156.
7. G. A. Borlase, N. Vlahopoulos, "An Energy Finite Element Optimization Process for Reducing High Frequency Vibration in Large Scale Structures," *Journal of Finite Element Analysis and Design*, Vol. 36, 2000, pp. 51-67.
8. W. Zhang, A. Wang, N. Vlahopoulos, and K. Wu, "High Frequency Vibration Analysis of Thin Elastic Plates under Heavy Fluid Loading by an Energy Finite Element Method," *Journal of Sound and Vibration*, Vol. 263(1), 22 May 2003, pp. 21-46
9. W. Zhang, A. Wang, and N. Vlahopoulos, "An Alternative Energy Finite Element Formulation based on Incoherent Orthogonal Waves and its Validation for Marine Structures," *Finite Elements in Analysis and Design*, Vol.38, 2002, pp. 1095-1113.
10. A. Wang, N. Vlahopoulos, K. Wu, "Development of an Energy Boundary Element Formulation for Computation of Sound Radiation at High Frequency," *Journal of Sound and Vibration*, Vol. 278, 2004, pp. 413-436.
11. W. Zhang, N. Vlahopoulos, K. Wu, "An Energy Finite Element Formulation for High Frequency Vibration Analysis of Externally Fluid-Loaded Cylindrical Shells with Periodic Circumferential Stiffeners subjected to Axi-Symmetric Excitation" accepted by *Journal of Sound and Vibration.*
12. W. Zhang, N. Vlahopoulos, K. Wu, "High Frequency Vibration Analysis of Stiffened Plates under Heavy Fluid Loading by an Energy Finite Element Analysis Formulation," submitted *Finite Elements in Analysis and Design.*
13. S. B. Hong, N. Vlahopoulos, "A Hybrid Finite Element Formulation for Analyzing Systems of Beams and Plates in the Mid-Frequency Range" Internoise 2002, Dearborn, MI.
14. S.B. Hong, N. Vlahopoulos, "A Hybrid Finite Element Formulation for a beam plate system," submitted to *Journal of Sound and Vibration.*
15. A. Wang, N. Vlahopoulos, K. Wu, "An Energy Boundary Element Formulation for Sound Radiation at High Frequencies, Internoise 2002, Dearborn, MI.
16. F. W. Grosveld, J. I. Prichard, R. D. Buehrle, and R. S. Pappa, "Finite Element Modeling of the NASA Langley Aluminum Test-bed Cylinder," AIAA 2002-2418, 8th AIAA/CEAS Aeroacoustics Conference, June 17-19, 2002, Breckenridge, Colorado.
17. M. L. Rumerman, "The effect of fluid loading on radiation efficiency," *J. Acoust. Soc. Am.* **111**, 75-79 (2002).
18. M. L. Rumerman, "Estimation of broadband acoustic power radiated from a turbulent boundary layer-driven reinforced finite plate section due to rib and boundary forces," *J. Acoust. Soc. Am.* **111**, 1274-1279 (2002).
19. C.Y.R. Cheng, A. F. Seybert, and T. W. Wu, "A Multi-domain Boundary Element Solution for Silencer and Muffler Performance Prediction," *Journal of Sound and Vibration*, Vol. 151, 1991, pp. 119-129.
20. T. Tanaka, T. Fujikawa, T. Abe, and H. Utsuno, "A Method for the Analytical Prediction of Insertion Loss of a Two-Dimensional Muffler Model Based on the Transfer Matrix Derived from the Boundary Element Method," *ASME Trans. J. Vib. Acoust. Stress Rel. Design*, Vol. 107, 1985, pp. 86-91.
21. A. F. Seybert, C.Y.R. Cheng, and T. W. Wu, "The solution of coupled Interior/Exterior Acoustic Problems Using the Boundary Element Method," *J. Acoust. Soc. Am.*, Vol. 88, 1990, pp. 1612-1618.